Hindawi
Advances in Civil Engineering
Volume 2021, Article ID 8897756, 8 pages
https://doi.org/10.1155/2021/8897756

Research Article

Bending-Induced Cross-Sectional Deformation of Cold-Formed Steel Channel-Section Beams

Liusi Dai and Wenfu He

Department of Civil Engineering, Shanghai University, Shanghai, China

Correspondence should be addressed to Wenfu He; howunfu@shu.edu.cn

Received 20 September 2020; Accepted 30 April 2021; Published 12 May 2021

Academic Editor: Weerachart Tangchirapat

In practice, the cold-formed steel structures are widely used, and their geometrical nonlinearity is of great significance in structural design. However, the current analytical solutions are only applied to linear problems, and the nonlinear problems are mostly considered by commercial finite element software. This paper presents an analytical model to describe the bending-induced cross-sectional deformation in cold-formed steel channel-section beams when subjected to transverse bending loads. The nonlinear effect of cross-sectional deformation on the relationship between the overall bending curvature and applied moment is examined. A parametric study is also carried out to examine how the flange width, lip length, and thickness of the section affect the cross-sectional deformation and corresponding nonlinear bending behavior of the beams.

1. Introduction

Thin-walled beams frequently exhibit flattened cross-sectional deformation when they are subjected to bending loads. A typical example is the ovalization of the cross-section of circular cylindrical shells of infinite length under pure bending, which was reported by Brazier in 1927 [1]. The cross-sectional flattening leads to a reduction of the overall bending stiffness of the shells, resulting in a nonlinear relationship between the curvature and applied moment. For the circular cylindrical shells of finite length, the ovalization of the cross-section is also affected by the length of the shells and the restraint conditions at the two ends of the shells [2]. The similar phenomenon of the flattened cross-sectional deformation has been also found in angle-section beams [3]; channel-section beams bent about the axis parallel to web line [4] and rectangular box-section beams [5], in which the bending-induced cross-sectional deformation leads to a reduction in the bending rigidity of the beams and thus results in a nonlinear relationship between the bending deflection and applied transverse load.

The flattened cross-sectional deformation observed in hat-section beams when subjected to bending is referred to as flange curling, which, in principle, is similar to the ovalization of the cross-section of circular cylindrical shells. When the flange curling is considered, the cross-section properties of the beam need to be calculated based on the deformed cross-section with curved geometry, representing the second-order effect. The phenomenon of flange curling was first reported by Winter in 1940 [6]. In Eurocode 3–Part 1.3 a formula is suggested to estimate the deformation caused by the flange curling [7]. Experimental investigation has been carried out on the flange curling in profiled steel decks with different slender geometries [8]. The results of the experiments were compared with those obtained using nonlinear finite element analysis method. Analytical models were also developed to study the flange curling phenomenon in wide flange trapezoidal panels [9] and wide single-flange steel panels [10]. The analytical calculation methods were demonstrated using experimentally obtained data.

Compared to hot-rolled steel beams, cold-formed steel beams may be even easier to exhibit cross-sectional deformation because of its thin thickness and open-section nature. To predict the effect of the cross-sectional deformation on the overall bending behavior of the beams, one has to know how individual segments deform within the cross-

section. In this paper, an analytical model is presented to describe the bending-induced flange deformation in cold-formed steel channel-section beams when subjected to transverse bending loads. The nonlinear effect of the local flange deformation within the cross-section on the relationship between the overall bending curvature and applied moment is examined. A parametric study is also carried out to examine how the flange width, lip length, and thickness of the section affect the cross-section deformation and corresponding nonlinear bending behavior of the beam.

2. Analytical Model Describing Flange Curling in Channel-Section Beams

When a beam is subjected to a pure bending, the bending stresses of the beam on the top and bottom layers are in opposite directions (see the stresses presented by dash lines in Figure 1). Beam curvature causes a vertical imbalance of the longitudinal tension and compression bending stresses. As it is shown in Figure 1, the combination of the two compressive stresses on the top layer and the two tensile stresses on the bottom layer leads to a vertical compression of the cross-section, which causes an in-plane flattening of the cross-section. For solid-section beams, the deformation generated by this vertical compression is negligible and thus there is no need to consider the flattening of the cross-section. However, for thin-walled open- or close-section beams, the deformation generated by the vertical compression may be significant and thus there is a need to consider the cross-sectional shape changing and/or the flattening deformation of the cross-section.

Herein, we consider a thin-walled, cold-formed steel channel-section beam with web depth h, flange width b, lip length c, and thickness t. Assume that the beam is subjected to a bending load and results in deflection $v(x)$ and bending compressive stress $\sigma(x)$ in its upper flange, where x is the longitudinal coordinate of the beam. The equivalent compressive forces in the upper flange and lip generated by the bending compressive stress thus are σbt and σct $(1 - c/h)$, respectively. For a beam element of length dx, the corresponding flattening force is σbtv"dx, which can be assumed to distribute uniformly on the upper flange over a surface area $b$dx, and σct $(1 - c/h)$ v"dx, which acts on the lip over a line length dx. Hence, the former provides a surface load of σtv" on the upper flange and the latter gives a line load of σct $(1-c/h)$ v" on the joint line between the upper flange and lip. The similar flattening forces can be also derived for the lower flange and lip, which are shown in Figure 2(a). The deformation of the cross-section of the beam under the action of the flattening forces can be calculated using a frame model, as shown in Figure 2(b), in which the web line is subjected a pure bending, and the upper and lower flanges are subjected to a uniformly distributed load plus a concentrated load acting at the lip. Based on the theory of plates and shells [11], the local deflection of the flange thus can be expressed as follows:

$$y(x, y) = \frac{\sigma \mathrm{tbh}}{4\,D}\left[b + 2c\left(1 - \frac{c}{h}\right)\right] Z \frac{\mathrm{d}^2 v}{\mathrm{d}x^2} + \frac{\sigma t}{24\,D} z^2 \left(6b^2 - 4bz + z^2\right) \frac{\mathrm{d}^2 v}{\mathrm{d}x^2} + \frac{\sigma \mathrm{tc}}{6\,D}\left(1 - \frac{c}{h}\right) z^2 (3b - z) \frac{\mathrm{d}^2 v}{\mathrm{d}x^2}, \tag{1}$$

where $D = \mathrm{Et3121}\text{-}\nu 2$ is the bending rigidity and z is the coordinate along with flange line, E is the Young's modulus, and ν is the Poisson's ratio. The first term in equation (1) is the deflection due to the web rotation; the 2nd and 3rd terms in equation (1) are caused by the uniform load on the flange and concentrated load on the lip, respectively [12]. Based on the theory of plates and shells [11], the deflection and rotation of the lip are expressed as follows:

$$\begin{aligned} y(x, b) &= \frac{\sigma \mathrm{tb}^2 h}{4\,D}\left[b + 2c\left(1 - \frac{c}{h}\right)\right] \frac{\mathrm{d}^2 v}{\mathrm{d}x^2} + \frac{\sigma \mathrm{tb}^4}{8\,D} \frac{\mathrm{d}^2 v}{\mathrm{d}x^2} + \frac{\sigma \mathrm{tcb}^3}{3\,D}\left(1 - \frac{c}{h}\right) \frac{\mathrm{d}^2 v}{\mathrm{d}x^2}, \\ \frac{\mathrm{d}y(x, b)}{\mathrm{d}z} &= \frac{\sigma \mathrm{tbh}}{4\,D}\left[b + 2c\left(1 - \frac{c}{h}\right)\right] \frac{\mathrm{d}^2 v}{\mathrm{d}x^2} + \frac{\sigma \mathrm{tb}^3}{6\,D} \frac{\mathrm{d}^2 v}{\mathrm{d}x^2} + \frac{\sigma \mathrm{tcb}^2}{2\,D}\left(1 - \frac{c}{h}\right) \frac{\mathrm{d}^2 v}{\mathrm{d}x^2}. \end{aligned} \tag{2}$$

The second moment of area of the deformed channel-section beam about its neutral axis thus can be calculated as follows:

$$I(x) = \frac{\mathrm{th}^3}{12} + 2t \int_o^b \left(\frac{h}{2} - y\right)^2 \mathrm{d}z + 2t\left[\frac{c^3}{12}\left(1 - \left(\frac{\mathrm{d}y(x, b)}{\mathrm{d}z}\right)^2\right) + c\left(\frac{h - c}{2} - y(x, b)\right)^2\right]. \tag{3}$$

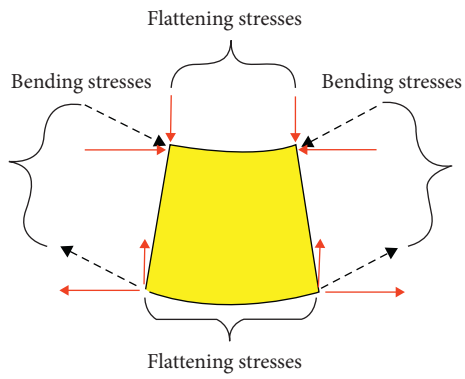

Figure 1: Cross-sectional flattening in beams induced by bending stresses.

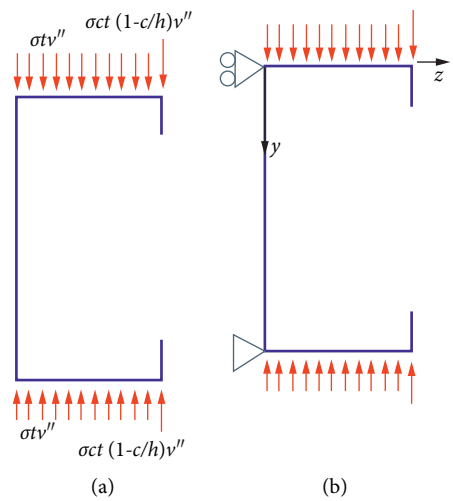

Figure 2: (a) Distribution of flattening forces in lipped flanges. (b) Simplified model used for calculating cross-sectional deformation in a channel-section beam.

For small local deformation, the second-order terms of $y(x, z)$ would be small and thus can be neglected. In this case, the reduction of the second moment of area caused by cross-sectional flattening can be approximated as follows:

$$\Delta I(x) = 2\mathrm{th}\int_o^b y\mathrm{d}z + 2\mathrm{tc}(h-c)y(x,b). \tag{4}$$

Substituting equations (1) and (2) into (5), it yields

$$\Delta I(x) = \frac{\sigma t^2 b^4 h^2}{4\,D}\frac{\mathrm{d}^2 v}{\mathrm{d}x^2}\left\{\left[1+\frac{2c}{b}\left(1-\frac{c}{h}\right)\right]^2+\frac{2b}{5h}+\frac{2c}{h}\left(1-\frac{c}{h}\right)+\frac{8c^2}{3\mathrm{bh}}\left(1-\frac{c}{h}\right)^2\right\}. \tag{5}$$

Note that the bending stress in the flanges can be expressed as

$$\sigma(x) = \frac{\mathrm{Eh}}{2}\frac{d^2 v}{dx^2}. \tag{6}$$

Substituting equation (6) into equation (5), it yields

$$\Delta I(x) = h^2\left(\frac{\mathrm{d}^2 v}{\mathrm{d}x^2}\right)^2\Delta I_o, \tag{7}$$

where ΔI_o is a section dimension-dependent parameter and is expressed as follows:

$$\Delta I_o = \frac{3\left(1-\nu^2\right)b^4 h}{2t}\left\{\left[1+\frac{2c}{b}\left(1-\frac{c}{h}\right)\right]^2+\frac{2b}{5h}+\frac{2c}{h}\left(1-\frac{c}{h}\right)+\frac{8c^2}{3\mathrm{bh}}\left(1-\frac{c}{h}\right)^2\right\}. \tag{8}$$

The bending equation of the channel-section beam established on the deformed framework can be expressed as follows:

$$E\left(I_o - \Delta I\right)\frac{\mathrm{d}^2 v}{\mathrm{d}x^2} = M(x), \tag{9}$$

where I_o is the second moment of area of the undeformed channel-section beam about its major axis and $M(x)$ is the internal moment of the beam. Since ΔI is the quadratic function of curvature, equation (9) is a nonlinear differential equation about the curvature. To solve these nonlinear differential equations, one has to use an approximate method or a numerical method. Assume the solution of equation (9) can be expressed as the sum of two parts, that is,

$$v(x) = v_o(x) + v_1(x), \tag{10}$$

where $v_o(x)$ is the deflection function without considering flange curling effect and $v_1(x)$ is the additional deflection function when the flange curling is taken into account. It is obvious that $v_o(x)$ can be determined from the classical bending theory of beams as follows:

$$\mathrm{EI}_o\frac{\mathrm{d}^2 v_o}{\mathrm{d}x^2} = M(x). \tag{11}$$

Substituting equation (10) into equation (9) and using equation (11) and noticing the fact that $v_1(x) \ll v_o(x)$, it yields

$$\mathrm{EI}_o\frac{\mathrm{d}^2 v_1}{\mathrm{d}x^2} = E\Delta I\frac{\mathrm{d}^2 v_o}{\mathrm{d}x^2} + E\Delta I\frac{\mathrm{d}^2 v_1}{\mathrm{d}x^2} \approx E\Delta I\frac{\mathrm{d}^2 v_o}{\mathrm{d}x^2} = \mathrm{Eh}^2\left(\frac{\mathrm{d}^2 v_o}{\mathrm{d}x^2}\right)^3\Delta I_o. \tag{12}$$

In equation (12), ΔI has been evaluated by using $v_o(x)$ only. Equation (12) indicates that the additional deflection function $v_1(x)$ is generated due to an equivalent moment expressed by the right-hand-side term of equation (12), which is proportional to $(\mathrm{d}^2 v_o/\mathrm{d}x^2)^3$. Hence, to find the solution of $v(x)$, we first find $v_o(x)$ from equation (11), then we approximate $\Delta I\ (x)$ using equation (7) and then the additional moment of $\mathrm{Eh}^2(\mathrm{d}^2 v_o/\mathrm{d}x^2)^3\Delta I_o$, and finally, we calculate $v_1(x)$ from equation (12).

3. Numerical Examples

Two examples are given herein to demonstrate the model developed above. One is the beam subjected to a pure bending, and the other is the beam subjected to a uniformly distributed load at shear centre. In both cases, the beam is assumed to be simply supported at its two ends and have the dimensions of beam length $l = 7000$ mm, web depth $h = 200$ mm, flange width $b = 75$ mm, lip length $c = 15$ mm, and section thicknesses $t = 1.5$ mm. The mechanical properties of the beam are Young's modulus $E = 200$ GPa, Poisson's ration $\nu = 0.3$, and yield stress $\sigma_y = 500$ MPa.

Example 1. For the beam subjected to a pure bending $M(x) = M_o$. The deflection function obtained by solving equation (12) can be expressed as follows:

$$v_o(x) = \frac{M_o l^2}{2\mathrm{EI}_o}\left[\left(\frac{x}{l}\right)^2 - \frac{x}{l}\right]. \tag{13}$$

Substituting equation (13) into equation (7), it yields

$$\Delta I(x) = \left(\frac{M_o h}{\mathrm{EI}_o}\right)^2\Delta I_o. \tag{14}$$

Substituting equation (13) into equation (12) and solving the differential equation, it yields

$$v_1(x) = \frac{\Delta I_o}{I_o}\left(\frac{M_o h}{\mathrm{EI}_o}\right)^2\left(\frac{M_o l^2}{2\mathrm{EI}_o}\right)\left[\left(\frac{x}{l}\right)^2 - \frac{x}{l}\right]. \tag{15}$$

Hence, the nonlinear deflection function of the beam when the flange curling is taken into account is expressed as

$$v(x) = v_o(x) + v_1(x) = \left(1 + \frac{\Delta I}{I_o}\right)v_o(x) = \left(\frac{M_o l^2}{2\mathrm{EI}_o}\right) \cdot \left[1 + \frac{\Delta I_o}{I_o}\left(\frac{M_o h}{\mathrm{EI}_o}\right)^2\right]\left[\left(\frac{x}{l}\right)^2 - \frac{x}{l}\right], \tag{16}$$

Figure 3 shows the variation of the deflection of the channel-section beam at mid-span with the applied moment, calculated using equations (13) and (16), in which the three straight lines and three curves represent the beams with three different flange widths. It can be seen from the figure that the three straight lines, obtained from the linear solution equation (13), coincide together for the three beams of different flange widths. This is because of the use of the dimensionless moment, M_o/M_y, in the plot. However, the three curves, obtained from the nonlinear solution equation (16), for the three beams of different flange widths, are different. For the same moment ratio, the wider the flange, the larger the deflection, indicating that the flange curling is more significant in the beams with wider flanges. Figure 4 shows the similar moment-deflection curves of the channel-section beams with three different section thicknesses. It is observed from the figure that the three linear solutions coincide together, whereas the three nonlinear solutions are slightly different. The thicker the section thickness is, the closer the corresponding nonlinear solution is to the linear solution, indicating the flange curling is less important in the beams with thicker section thickness. Figure 5 shows the moment-deflection curves of the channel-section beams with three different lip lengths. It can be seen from the figure that the lip length has a considerable influence on flange curling of channel-section beam. The effects of nonlinearity are more significant as the lip length increases. Similar to those shown in Figures 3 and 4, all three linear solutions come together, but three nonlinear solutions are dispersed. The longer the lip length is, the more the nonlinear solution is different from the linear solution, indicating that the flange curling is more n the beams with longer lip lengths.

Example 2. For the beam subjected to a uniformly distributed transverse load, $M(x) = \mathrm{qx}/2(l - x) = 4\ M_o[(x/l) - (x/l)^2]$, where q is the loading density and $M_o = \mathrm{ql}^2/8$ is the

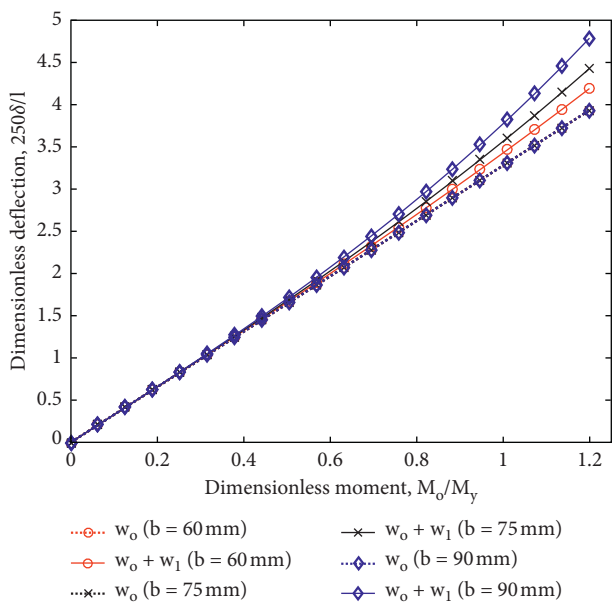

Figure 3: Effect of flange width on flange curling of channel-section beam ($l = 7000$ mm, $h = 200$ mm, $c = 15$ mm, and $t = 1.5$ mm) (solid lines are nonlinear solution with flange curling; dash lines are linear solution without flange curling).

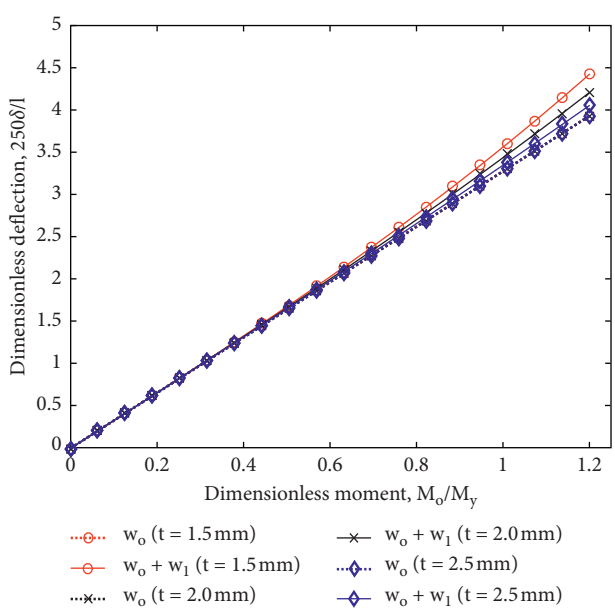

Figure 4: Effect of section thickness on flange curling of channel-section beam ($l = 7000$ mm, $h = 200$ mm, $b = 75$ mm, and $c = 15$ mm) (solid lines are nonlinear solution with flange curling; dash lines are linear solution without flange curling).

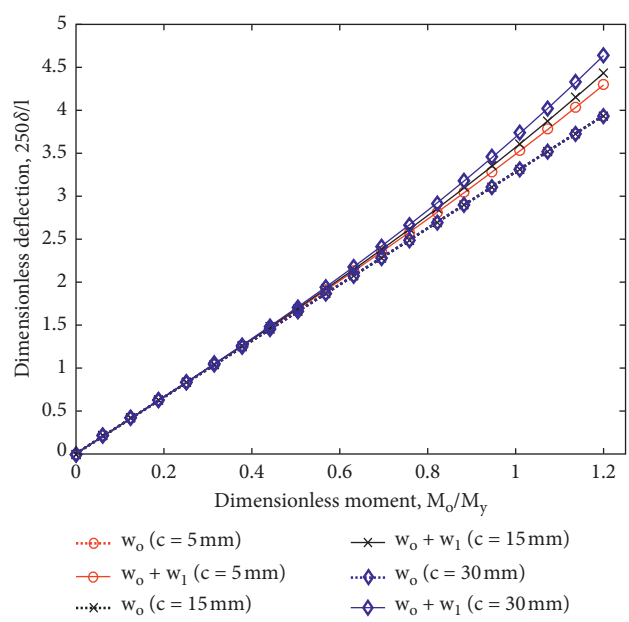

Figure 5: Effect of lip length on flange curling of channel-section beam ($l = 7000$ mm, $h = 200$ mm, $b = 75$ mm, and $t = 1.5$ mm) (solid lines are nonlinear solution with flange curling; dash lines are linear solution without flange curling).

maximum moment occurring at the mid-span of the beam. The deflection function $v_o(x)$ can be obtained by solving equation (11) and is expressed as follows:

$$v_o(x) = \frac{M_o l^2}{3\mathrm{EI}_o}\left[2\left(\frac{x}{l}\right)^3 - \left(\frac{x}{l}\right)^4 - \frac{x}{l}\right]. \tag{17}$$

Substituting equation (17) into equation (7), it yields

$$\Delta I(x) = \left(\frac{4M_o h}{\mathrm{EI}_o}\right)^2 \left[\frac{x}{l} - \left(\frac{x}{l}\right)^2\right]^2 \Delta I_o. \tag{18}$$

Substituting equation (18) into equation (12) and solving the differential equation, it yields

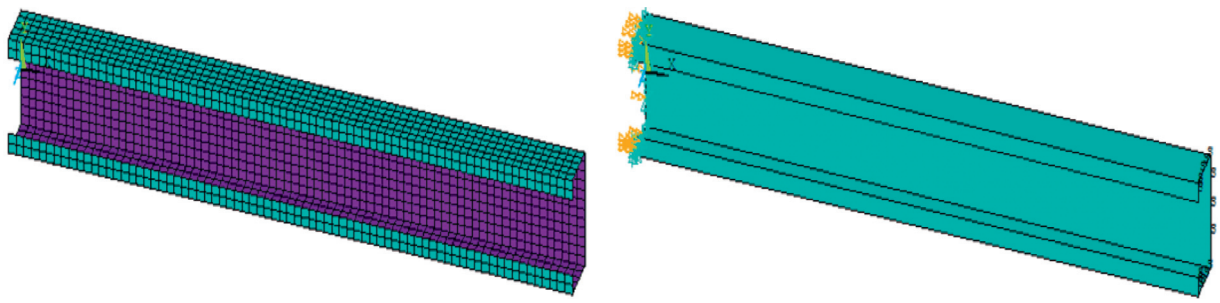

(a) (b)

Figure 6: (a) Finite element mesh and (b) boundary conditions used in the analysis.

$$v_1(x) = \frac{\Delta I_o}{I_o}\left(\frac{4M_o h}{\mathrm{EI}_o}\right)^2\left(\frac{M_o l^2}{\mathrm{EI}_o}\right)\left[\frac{1}{5}\left(\frac{x}{l}\right)^5 - \frac{2}{5}\left(\frac{x}{l}\right)^6 + \frac{2}{7}\left(\frac{x}{l}\right)^7 - \frac{1}{14}\left(\frac{x}{l}\right)^8 - \frac{1}{70}\frac{x}{l}\right]. \tag{19}$$

Hence, the nonlinear deflection function of the beam when the flange curling is taken into account is expressed as

$$\begin{aligned} v(x) = v_o(x) + v_1(x) &= \frac{M_o l^2}{3\mathrm{EI}_o}\left[2\left(\frac{x}{l}\right)^3 - \left(\frac{x}{l}\right)^4 - \frac{x}{l}\right] \\ &+ \frac{\Delta I}{I_o}\left(\frac{4M_o h}{\mathrm{EI}_o}\right)^2\left(\frac{M_o l^2}{\mathrm{EI}_o}\right)\left[\frac{1}{5}\left(\frac{x}{l}\right)^5 - \frac{2}{7}\left(\frac{x}{l}\right)^7 - \frac{1}{14}\left(\frac{x}{l}\right)^8 - \frac{1}{70}\frac{x}{l}\right]. \end{aligned} \tag{20}$$

The maximum deflection at the mid of the beam, where $x = l/2$, can be expressed as follows:

$$v\left(\frac{l}{2}\right) = v_o\left(\frac{l}{2}\right) + v_1\left(\frac{l}{2}\right) = \frac{5M_o l^2}{48\mathrm{EI}_o}\left[1 + \frac{279}{350}\left(\frac{\Delta I_o}{I_o}\right)\left(\frac{M_o h}{\mathrm{EI}_o}\right)^2\right]. \tag{21}$$

Comparing equation (21) with equation (16), it is obvious that the flange curling in the beam with a uniformly distributed load is very similar to that in the beam under pure bending. Only difference is the precoefficient of the nonlinear term, which is 279/350 instead of 1.0 in the beam under the pure bending, indicating that the flange curling in the former would be slightly larger than that in the latter.

Furthermore, the nonlinear finite element analysis method [13–15] is used to demonstrate the present analytical model. The finite element model of the channel-section beam under pure bending is established using ANSYS software. Considering the beam is symmetric about its mid-section, only half of the beam length is modelled in the finite element analysis. Figure 6 shows the finite element mesh of the half beam and corresponding boundary conditions employed in the analysis. The analysis is performed using 4-noded thin shell elements with a maximum element size not exceeding 10 mm, the choice of which is based on our previous study on the similar analysis [16–18]. The boundary conditions are assumed as that all nodes on the symmetric section ($x = l/2$) have zero axial displacement and zero rotations about lateral and transverse axes, and all nodes on the end section ($x = 0$) have zero lateral and transverse displacements and zero rotation about longitudinal axis. To apply the pure bending, a fictitious rigid plate is used to cover the end section, on which a concentrated moment is applied. To avoid the lateral-torsional buckling of the beam, the lateral displacement of the upper and lower flanges is restrained in the analysis. Linear elastic material model is used in the analysis with Young's modulus $E = 200$ GPa and Poisson's ration $\nu = 0.3$. In other words, it is only the geometric nonlinearity that is considered in the analysis.

Figure 7 shows the comparison of the moment-deflection curves obtained from the nonlinear finite element analysis and presents analytical model for two channel-section beams. It can be seen from the figure that the moment-deflection curves provided by the present model are very close to those predicted by the nonlinear finite element analysis, indicating that the present approach for modelling flange curling is adequate, although it is very simple.

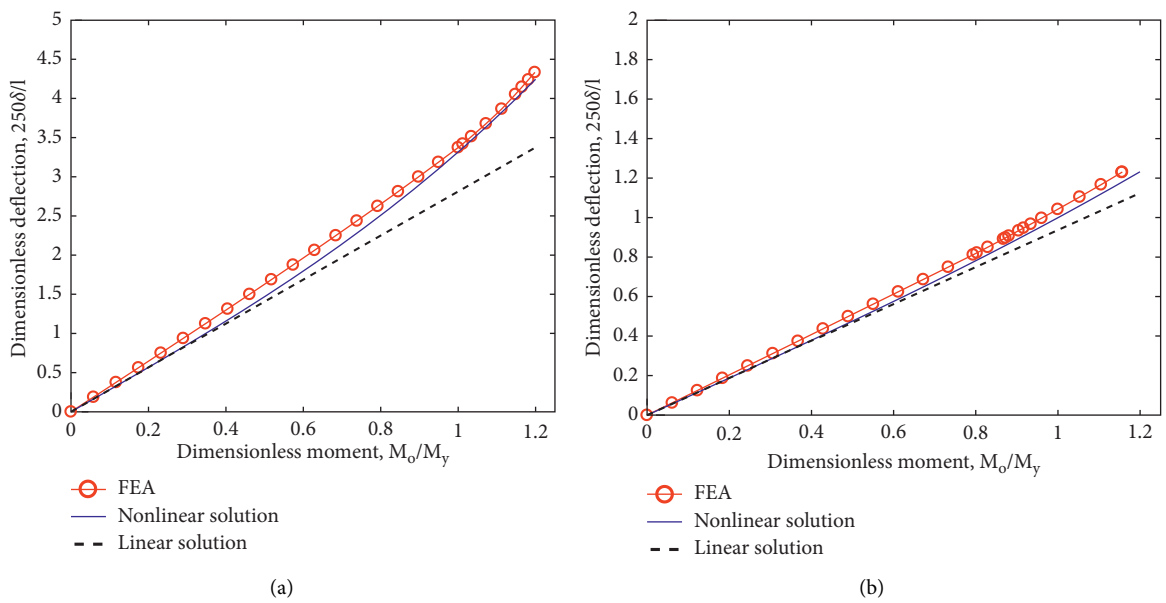

Figure 7: Comparison of moment-deflection curves obtained from the nonlinear finite element analysis and the present analytical model for two channel-section beams of length $l = 3000$ mm (Section 1: $h = 100$ mm, $b = 50$ mm, $c = 20$ mm, and $t = 1.0$ mm; Section 2: $h = 300$ mm, $b = 90$ mm, $c = 30$ mm, and $t = 2.0$ mm). (a) Section 1. (b) Section 2.

4. Conclusions

Cold-formed steel beams have been increasingly used in buildings and other load-carrying structures. Due to thin thickness cold-formed steel beams may exhibit cross-sectional deformation when they are subjected to bending loadings, the interaction between the transverse bending of the beam and the in-plane flattening of the beam cross-section leads the beams to have a nonlinear bending behavior. In this paper, an analytical model has been developed to describe the interactive effect between the bending and flattening for lipped channel-section beams. The present model has been demonstrated by using nonlinear finite element analysis results. From the present study, the following conclusions can be drawn:

(i) The cross-sectional deformation in channel-section beams when subjected to transverse bending loadings is mainly caused by the flange curling, which results in a reduction of the overall flexural rigidity of the beams.

(ii) The remarkable flange curling mainly occurs in the channel-section beams, which have wide flanges, long lips, and thin thickness, and the greater flange curling occurs with higher bending stresses.

(iii) The magnitude of flange curling occurred in lipped channel-section beams increases with the increase of flange width or lip length, but decreases with increased section thickness.

(iv) The flange curling results in an increase of the bending deflection of the beam and the nonlinear deflection may be significantly different from that calculated using the linear bending theory of beams.

Data Availability

The data used to support the findings of this study are included within the article.

Conflicts of Interest

No potential conflicts of interest were reported by the authors.

Acknowledgments

The first author would like to acknowledge the financial support provided by the National Natural Science Foundation of China (no. 51908347).

References

[1] L. G. Brazier, "On the flexure of thin cylindrical shells and other "thin" sections," *Proceedings of the Royal Society of London. Series A, Containing Papers of a Mathematical and Physical Character*, vol. 116, no. 773, pp. 104–114, 1927.

[2] L.-Y. Li and R. Kettle, "Nonlinear bending response and buckling of ring-stiffened cylindrical shells under pure bending," *International Journal of Solids and Structures*, vol. 39, no. 3, pp. 765–781, 2002.

[3] W.-B. Yuan, "Geometric nonlinear bending response and buckling of angle-section beams under pure bending," *Journal of Constructional Steel Research*, vol. 85, pp. 73–80, 2013.

[4] W.-B. Yuan, "Nonlinear instability analyses of channel-section beams subjected to minor-axis pure bending," *International Journal of Mechanical Sciences*, vol. 73, pp. 77–81, 2013.

[5] W.-B. Yuan, Z.-S. Bao, N.-T. Yu, S.-S. Zhu, and L.-P. Wu, "Nonlinear bending of box section beams of finite length under uniformly distributed loading," *International Journal of Steel Structures*, vol. 17, no. 2, pp. 491–499, 2017.

[6] G. Winter, "Stress distributions in and equivalent width of flanges of wide, thin-wall steel beams, Technical notes," *National Advisory Committee for Aeronautics*, vol. 784, pp. 1–27, 1940.

[7] European Committee for Standardization, *EN 1993-1-3, Eurocode 3: Design of Steel Structures. Part 1–3: General Rules. Supplementary Rules for Cold-Formed Thin Gauge Members and Sheeting*, European Committee for Standardization, Brussels, Belgium, 2006.

[8] E. S. Bernard, R. Q. Bridge, and G. J. Hancock, "Flang curling in profiled steel decks," *Thin-walled Structures*, vol. 25, no. 1, pp. 1–29, 1996.

[9] N. Silvestre, "Analytical model to study the curling phenomena in wide flange trapezoidal panels," *Engineering Structures*, vol. 29, no. 12, pp. 3443–3454, 2007.

[10] N. Silvestre, "Non-linear curling of wide single-flange steel panels," *Journal of Constructional Steel Research*, vol. 65, no. 3, pp. 509–522, 2009.

[11] S. P. Timoshenko and S. Woinowsky-Krieger, *Theory of Plates and Shells*, McGraw-Hill, New York, NY, USA, 1959.

[12] L.-Y. Li, "Analyses of distortional buckling of cold-formed sigma purlins using EN1993-1-3," *Journal of Constructional Steel Research*, vol. 65, no. 12, pp. 2099–2102, 2009.

[13] A. Bakoura, F. Bourada, A. A. Bousahla et al., "Buckling analysis of functionally graded plates using HSDT in conjunction with the stress function method," *Computers and Concrete*, vol. 27, no. 1, pp. 73–83, 2021.

[14] N. Bendenia, M. Zidour, A. A. Bousahla et al., "Deflections, stresses and free vibration studies of FG-CNT reinforced sandwich plates resting on Pasternak elastic foundation," *Computers and Concrete*, vol. 26, no. 3, pp. 213–226, 2020.

[15] A. Menasria, A. Kaci, A. A. Bousahla et al., "A four-unknown refined plate theory for dynamic analysis of FG-sandwich plates under various boundary conditions," *Steel and Composite Structures*, vol. 36, no. 3, pp. 355–367, 2020.

[16] C. Ren, L.-Y. Li, and J. Yang, "Bending analysis of partially restrained channel-section purlins subjected to up-lift loadings," *Journal of Constructional Steel Research*, vol. 72, pp. 254–260, 2012.

[17] J. Zhu, J.-K. Chen, and C. Ren, "Numerical study on the moment capacity of zed-section purlins under uplift loading," *Structural Engineering and Mechanics*, vol. 49, no. 2, pp. 147–161, 2014.

[18] C. Ren, B. Wang, and X. Zhao, "Numerical predictions of distortional-global buckling interaction of perforated rack uprights in compression," *Thin-Walled Structures*, vol. 136, pp. 292–301, 2019.